Journal of Applied Mechanics and Technical Physics, Vol. 42, No. 6, pp. 991–996, 2001

HYDROELASTIC BEHAVIOR OF A FLOATING PLATE IN WAVES

L. A. Tkacheva

UDC 532.591

The behavior of a floating semi-infinite plate in surface waves incident normally to the edge of the plate is studied. We used an analytical solution of this problem obtained earlier by the Wiener–Hopf technique. In this paper, we study the distributions of displacements, deformations, and pressure over the plate as functions of the dimensionless parameters of the problem (reduced rigidity and depth) and their asymptotic distributions for large and small wavelengths.

The model of a floating elastic plate has been used previously in studies of the behavior of an ice sheet [1, 2]. At present, this problem is of interest in connection with the design of artificial islands and floating platforms used for various purposes. Existing numerical methods yield reliable results only for large and intermediate wavelengths and are inadequate for short incident waves. There are a number of analytical solutions for a semi-infinite plate obtained by the Wiener–Hopf technique [3–6]. However, in all the paper cited, the solution depends on two constants, which are determined from a system of linear algebraic equations. The coefficients of the system have a complicated form. In [7], the system was solved, an analytical solution for normal wave incidence on a plate in a liquid of finite depth was obtained by the Wiener–Hopf technique, and simple exact formulas for reflection and transmission coefficients and an expression for the velocity potential were derived. However, in [7], we studied only the far field. The present paper focuses on the behavior of the plate: distributions of displacements, strains, and pressure over the plate. Similar results for an infinitely deep liquid are presented in [8].

Formulation of the Problem. We consider the potential flow of an ideal incompressible liquid of depth H. The surface of the liquid is partly covered with a semi-infinite thin elastic plate, and the rest of the liquid is free. A plane progressive wave of small amplitude propagates at right angle to the edge of the plate, and the wavelength far exceeds the plate thickness. The problem is solved in a linear approach. We introduce Cartesian coordinates (x, y) with the origin O at the plate edge, and the Ox axis directed along the plate perpendicular to its edge. The draught of the plate is neglected so that the boundary conditions are displaced to the undisturbed free-surface level. The velocity potential φ satisfies the Laplace equation $\Delta\varphi = 0$ $(-H < y < 0)$.

Let us introduce the following dimensionless variables: $\varphi' = \varphi/(A\sqrt{gl})$, $x' = x/l$, $y' = y/l$, $t' = \omega t$, $p' = p/(\rho g A)$, $H' = H/l$, and $l = g/\omega^2$. Here A is the incident-wave amplitude, l is the characteristic length, g is the acceleration due to gravity, t is time, p is the pressure, ρ is the density of the liquid, and ω is the frequency of the incident wave. Below, the primes are omitted. The dependence of all functions on time in dimensionless variables is determined by the multiplier e^{-it}. The potential φ is written as

$$\varphi = \varphi_0 + \varphi_1, \qquad \varphi_0 = \mathrm{e}^{i\gamma x}\cosh\left(\gamma(y+H)\right)/\cosh\left(\gamma H\right),$$

where φ_0 is the potential of the incident wave, φ_1 is the diffraction potential, and γ is the wavenumber satisfying the dispersion relation for surface waves: $\gamma\tanh\left(\gamma H\right) - 1 = 0$. Then, we can formulate the following boundary-value problem for the potential φ_1 [7]:

$$\Delta\varphi_1 = 0 \qquad (-H < y < 0, \quad -\infty < x < \infty),$$

$$\frac{\partial\varphi_1}{\partial y} = 0 \qquad (y = -H, \quad -\infty < x < \infty);$$

Lavrent'ev Institute of Hydrodynamics, Siberian Division, Russian Academy of Sciences, Novosibirsk 630090.
Translated from Prikladnaya Mekhanika i Tekhnicheskaya Fizika, Vol. 42, No. 6, pp. 79–85, November–December, 2001. Original article submitted May 15, 2001.

0021-8944/01/4206-0991 $25.00

$$\frac{\partial\varphi_1}{\partial y} - \varphi_1 = 0 \qquad (y = 0, \quad x < 0); \tag{1}$$

$$\Big(\beta\,\frac{\partial^4}{\partial x^4} + 1 - \delta\Big)\frac{\partial\varphi_1}{\partial y} - \varphi_1 = B\mathrm{e}^{i\gamma x} \qquad (y = 0, \quad x > 0); \tag{2}$$

$$\frac{\partial^2}{\partial x^2}\,\frac{\partial\varphi}{\partial y} = \frac{\partial^3}{\partial x^3}\,\frac{\partial\varphi}{\partial y} = 0 \qquad (x = 0, \quad y = 0).$$

Here $\beta = D/(\rho g l^4)$ and $\delta = \rho_0 h/(\rho l)$ are dimensionless parameters of the problem, ρ_0 and h are the density and thickness of the plate, respectively, and $B = \delta - \beta\gamma^4$. In addition, the radiation conditions at the limit as $|x| \to \infty$ and the regularity conditions at the plate edge must be satisfied, i.e., the energy must be limited locally. The above assumptions imply that $\delta \ll 1$. Below, the value of δ is set equal to zero.

Analytical Solution of the Problem. An analytical solution of the problem for the potential φ_1 was obtained by the Wiener–Hopf technique in [7]. We introduce the dispersion functions $K_1(\alpha)$ for the free water surface and $K_2(\alpha)$ for the water under the plate. From boundary conditions (1) and (2), we find that for the free water surface, the dispersion function has the form $K_1(\alpha) = \alpha\tanh(\alpha H) - 1$ and for the liquid under the plate, it is written as $K_2(\alpha) = (\beta\alpha^4 + 1)\alpha\tanh(\alpha H) - 1$. The dispersion function for water has real roots $\pm\gamma$ and a countable set of purely imaginary roots $\pm\gamma_j$ $(j = 1, 2, \ldots)$, which are symmetric about the real axis. The second dispersion relation (for the liquid under the plate) has two real roots $\pm\alpha_0$, four complex roots $\pm\alpha_{-1}$ and $\pm\alpha_{-2}$, and a countable set of purely imaginary roots $\pm\alpha_j$ $(j = 1, 2, \ldots)$. The root α_{-1} is located in the first quadrant, and the root α_{-2} is located in the second quadrant; $\alpha_{-2} = -\bar{\alpha}_{-1}$.

Let us consider one-sided Fourier transforms for the diffraction potential φ_1:

$$\Phi_+(\alpha, y) = \int\limits_0^\infty \mathrm{e}^{i\alpha x}\varphi_1(x, y)\,dx, \qquad \Phi_-(\alpha, y) = \int\limits_{-\infty}^0 \mathrm{e}^{i\alpha x}\varphi_1(x, y)\,dx.$$

As was shown in [7], Φ_+ and Φ_- are analytic in the regions S_+ and S_-, respectively (S_+ is the half-plane $\operatorname{Im}\alpha > -c$ with cuts that exclude the points $-\alpha_0$ and $-\gamma$, S_- is the half-plane $\operatorname{Im}\alpha < c$ with cuts that exclude the points α_0 and γ, and the value of c corresponds to the smallest imaginary set of roots α_{-1}, α_1 [7, Fig. 3]).

Let us introduce the function $K(\alpha) = K_1(\alpha)/K_2(\alpha)$. Following the Wiener–Hopf technique, we must factorize the function $K(\alpha)$, i.e., write it as $K(\alpha) = K_+(\alpha)K_-(\alpha)$ [the functions $K_+(\alpha)$ and $K_-(\alpha)$ are regular in the regions S_+ and S_-, respectively]. We define the functions $K_\pm(\alpha)$ by the following expressions [7]:

$$K_\pm(\alpha) = \frac{(\alpha \pm \gamma)g_\pm(\alpha)}{\sqrt{\beta}(\alpha \pm \alpha_0)(\alpha \pm \alpha_{-1})(\alpha \pm \alpha_{-2})}, \qquad g_\pm(\alpha) = \exp\Big(\pm\frac{1}{2\pi i}\int\limits_{-\infty\mp id}^{\infty\mp id}\frac{\ln g(x)}{x - \alpha}\,dx\Big), \quad d < c,$$

$$g(x) = K(x)\beta(x^2 - \alpha_0^2)(x^2 - \alpha_{-1}^2)(x^2 - \alpha_{-2}^2)/(x^2 - \gamma^2).$$

In [7], for the velocity potential φ, we obtained the representations

$$\varphi(x, y) = \mathrm{e}^{i\gamma x}\,\frac{\cosh(\gamma(y + H))}{\cosh(\gamma H)} - \frac{BK_-(-\gamma)}{2\pi i\gamma^2}\int\limits_{-\infty}^{\infty}\mathrm{e}^{-i\alpha x}\frac{\cosh(\alpha(y + H))K_+(\alpha)\alpha^2}{\cosh(\alpha H)(\gamma + \alpha)K_1(\alpha)}\,d\alpha; \tag{3}$$

$$\varphi(x, y) = \mathrm{e}^{i\gamma x}\frac{\cosh(\gamma(y + H))}{\cosh(\gamma H)} - \frac{BK_-(-\gamma)}{2\pi i\gamma^2}\int\limits_{-\infty}^{\infty}\mathrm{e}^{-i\alpha x}\frac{\cosh(\alpha(y + H))\alpha^2}{\cosh(\alpha H)K_-(\alpha)(\gamma + \alpha)K_2(\alpha)}\,d\alpha. \tag{4}$$

The integration contour is entirely in the domain of intersection of the regions S_+ and S_-.

Plate Deflection and Elevation of the Free Boundary. The vertical displacement of the upper surface of the liquid is calculated by the formula $\eta_t = \varphi_y$ [7]. Hence, we have $\eta(x) = i\varphi_y(x, 0)$.

Let $\eta_+(x)$ be the vertical plate displacement. Using representation (4), we obtain

$$\eta_+(x) = i\mathrm{e}^{i\gamma x} + \frac{\beta\gamma^2 K_-(-\gamma)}{2\pi}\int\limits_{-\infty}^{\infty}\mathrm{e}^{-i\alpha x}\frac{\alpha^3\tanh(\alpha H)}{K_-(\alpha)(\gamma + \alpha)K_2(\alpha)}\,d\alpha.$$

The integrand is analytic in the lower half-plane except in the poles at $-\gamma$ and $-\alpha_j$ ($j = -2, -1, 0, \ldots$). The residue at the point $-\gamma$ is compensated for by the incident wave. Hence,

$$\eta_+(x) = -i\beta\gamma^2 K_-(-\gamma) \sum_{j=-2}^{\infty} \mathrm{e}^{i\alpha_j x} \frac{\alpha_j^3 \tanh(\alpha_j H)}{(\gamma - \alpha_j) K_-(-\alpha_j) K_2'(-\alpha_j)}. \tag{5}$$

As follows from Eq. (5), the vertical displacements of the plate are caused by a transmitted wave with wavenumber α_0 and edge effects, which decay exponentially away from the edge. We note that in a liquid of infinite depth, edge effects decay in proportion to x^{-4} [8].

The wavelength in the plate λ in dimensionless variables is defined by the formula $\lambda = 2\pi/\alpha_0$. At $\beta \ll 1$, $\alpha_0 \simeq \gamma$ and the wavelength in the plate is the same as that of the incident wave. With increase in β, the value of α_0 decreases, and the wavelength in the plate increases. As $\beta \to \infty$ (this case corresponds to short incident waves), $\alpha_0 \to 0$. In dimensional variables, the wavelength in the plate is $2\pi l/\alpha_0$. Let us introduce the characteristic length $L = (D/(\rho g))^{1/4}$ [9]. Because $\alpha_0 \sim (\beta H)^{-1/6}$ as $\beta \to \infty$, the wavelength in the plate has order $O(l^{1/3} L^{2/3} H^{1/6})$. Thus, as $\beta \to \infty$, the wavelength in the plate tends to zero.

After the substitution $\alpha_j^3 \tanh(\alpha_j H) = -K_1(\alpha_j)/(\beta\alpha_j^2)$ in Eq. (5), we write the expression obtained as an integral. Then, for the edge displacement, we obtain

$$\eta_+(0) = \frac{\beta\gamma^2 K_-(-\gamma)}{2\pi} \int\limits_{-\infty}^{\infty} \frac{K_1(\alpha)}{\alpha^2 K_-(\alpha)(\gamma + \alpha) K_2(\alpha)}\, d\alpha = \frac{\beta\gamma^2 K_-(-\gamma)}{2\pi} \int\limits_{-\infty}^{\infty} \frac{K_+(\alpha)}{\alpha^2(\gamma + \alpha)}\, d\alpha.$$

The integration contour selected on the real axis is passing below the points $\alpha_0, 0$, and γ and above the points $-\alpha_0$ and $-\gamma$. The last integral is calculated using the theory of residues. The integrand is analytic in the upper half-plane except in the multiple pole at zero. We obtain a simple formula for the vertical displacement of the plate edge:

$$\eta_+(0) = i\beta\gamma K_+(\gamma)[K_+'(0) - K_+(0)/\gamma]. \tag{6}$$

Since $K(0) = 1$ and $K_+(\alpha) = K_-(-\alpha)$, we have $K_+(0) = K_-(0) = 1$. Then, Eq. (6) is written as

$$\eta_+(0) = i\beta K_+(\gamma)[\gamma K_+'(0) - 1].$$

The elevation of the free boundary $\eta_-(x)$ is found using representation (3):

$$\eta_-(x) = i\mathrm{e}^{i\gamma x} + \frac{\beta\gamma^2 K_-(-\gamma)}{2\pi} \int\limits_{-\infty}^{\infty} \mathrm{e}^{-i\alpha x} \frac{\alpha^3 \tanh(\alpha H) K_+(\alpha)}{(\gamma + \alpha) K_1(\alpha)}\, d\alpha.$$

The integrand is analytic in the upper half-plane except in the poles at γ and γ_k ($k = 1, 2, \ldots$). As $K_-(-\alpha) = K_+(\alpha)$, we have

$$\eta_-(x) = i\mathrm{e}^{i\gamma x} + \frac{i\beta K_+^2(\gamma)}{2K_1'(\gamma)}\, \mathrm{e}^{-i\gamma x} + i\beta\gamma^2 K_+(\gamma) \sum_{j=1}^{\infty} \mathrm{e}^{-|\gamma_j| x} \frac{\gamma_j^2 K_+(\gamma_j)}{(\gamma + \gamma_j) K_1'(\gamma_j)}. \tag{7}$$

In (7), the first term represents an incident wave, the second term represents a reflected wave, and the remaining terms correspond to the edge effects (modes that decay exponentially away from the edge).

The distributions of plate displacement and free-boundary elevation with variation of the parameter β were studied numerically. For all values of β, maximum displacements of the plate occur near the edge. The calculations showed that for all values of β, the edge effects decay rather rapidly, so that at a distance of half as much again the transmitted wavelength, the correction for the edge effects does not exceed 0.1%. Figure 1 shows distributions of plate displacements along the x axis for various values of β and H. For $\beta = 10^{-4}$, the curves corresponding to $H = 1$ and 100 coincide. As can be seen from Fig. 1, the effect of the liquid depth on plate displacements is insignificant.

The vertical displacements of the upper boundary have a discontinuity at the edge, which indicates that the vertical displacement of the plate edge and the elevation of the free boundary at the edge are different. Figure 2 shows curves of displacement amplitudes of the plate edge $|\eta_+|$ and elevation of the free boundary at the edge $|\eta_-|$ versus β. For small values of β (corresponding to small rigidity of the plate or long incident waves), the plate behaves as a thin film and practically does not affect wave propagation; the plate oscillation amplitudes are close to unity. With increase in β, the amplitude of plate edge oscillations grows and reaches a maximum after which it

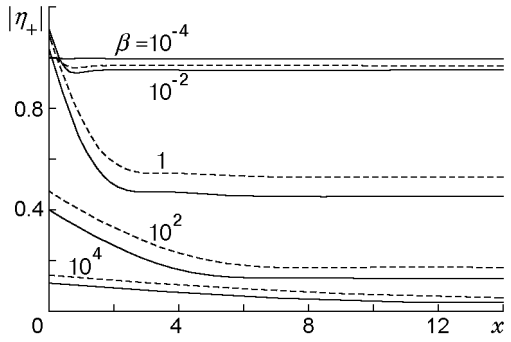

Fig. 1. Distribution of the amplitudes of plate displacements $|\eta_+|$ along x for different values of β: solid and dashed curves correspond to $H = 1$ and 100, respectively.

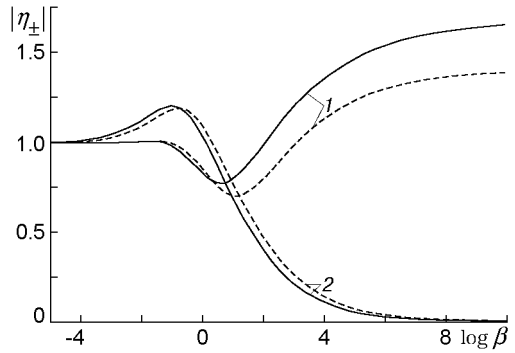

Fig. 2

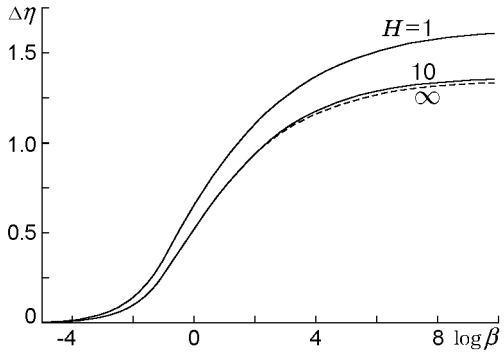

Fig. 3

Fig. 2. Amplitudes of free-boundary elevation at the edge $|\eta_-|$ (curves 1) and amplitudes of displacements of the plate edge $|\eta_+|$ (curves 2) versus β: solid and dashed curves refer to $H = 1$ and 100, respectively.

Fig. 3. Amplitudes of the level difference $\Delta\eta$ versus β: solid curves refer to $H = 1$ and 10 and the dashed curve refers to $H = \infty$.

decreases monotonically and tends to zero as $\beta \to \infty$ (large values of β correspond to a very rigid plate or short incident waves).

The amplitude of liquid oscillations at the edge is almost equal to unity for $\beta < 0.1$. With increase in β, it starts decreasing and reaches a minimum, after which it grows monotonically and reaches the asymptotic value corresponding to an absolutely rigid plate. A comparison of the diagrams shows that the depth of the liquid has a stronger effect on the liquid oscillation amplitude than on the plate oscillation amplitude. For small values of β, the oscillation amplitude of the plate edge is larger than the oscillation amplitude of the liquid at the edge. For large values of β, the plate practically does not oscillate, while the liquid oscillation amplitude is maximal.

Figure 3 shows the amplitudes of the difference in level between the plate and the liquid at the edge versus β for $H = 1$, 10, and ∞ [8]. At small depth, the amplitude of liquid oscillations increases. With increase in β, the amplitude of the level difference increases monotonically. If the plate thickness is smaller than the amplitude of the level difference, the plate edge periodically comes out of the water and impacts on it. In this case, the water impact should be taken into account, and another model must be used to describe this phenomenon.

Plate Strains. The plate strains are calculated from the formula $e_{xx} = -h\eta''(x)/2$. The plate strain amplitude in dimensionless variables is written as [7]

$$e_{xx} = Ahe(x)/(2l^2), \qquad e(x) = \eta''(x).$$

Distributions of dimensionless strain amplitudes $e(x)$ over the plate for various values of β are given in Fig. 4. Due to the boundary condition, the strains at the edge are equal to zero, and at a certain distance from the edge, the strain amplitude reaches a maximum and then decreases to a corresponding value in the transmitted wave. The strain amplitudes depend strongly on the liquid depth only for the small values of β and H. This is because the wavenumber α_0 depends strongly on the depth only for small values of β and H, and $\alpha_0 \to \infty$ as $H \to 0$.

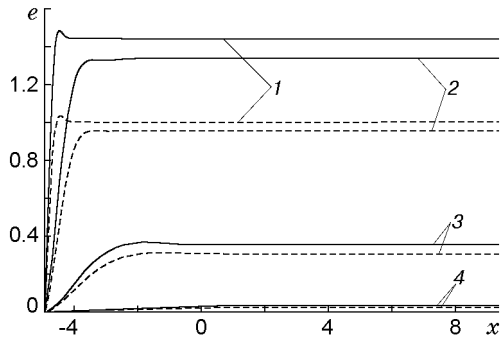

Fig. 4. Distributions of dimensionless strain amplitudes $e(x)$ for $\beta = 10^{-4}$ (1), 10^{-2} (2), 1 (3), and 10^2 (4): solid and dashed curves refer to $H = 1$ and 100.

TABLE 1

Dimensionless Coordinates of the Maximum Strain Points on the Plate

H	log β												
	-5	-4	-3	-2	-1	0	1	2	3	4	5	6	7
1	0.04	0.09	0.16	0.60	∞	0.45	0.46	0.47	0.47	0.47	0.47	0.48	0.48
∞	0.05	0.08	0.13	0.51	1.9	0.45	0.45	0.45	0.45	0.44	0.44	0.44	0.43

Table 1 gives dimensionless coordinates of the maximum strain points on the plate (normalized by the length of the transmitted wave $\lambda = 2\pi l/\alpha_0$) for different values of β at $H = 1$ and ∞ [8]. These are the maximum stress points (at these points, fractures and cracks are most probable) located rather close to the plate edge. In some ranges of values of β, the location of these points changes abruptly: $-1.5 < \log\beta < -1$ for $H = 1$ and $-1 \leqslant \log\beta < -0.75$ for $H = \infty$. In these ranges, the ratio of the maximum strain amplitude to the strain amplitude in the transmitted wave is insignificant. Hence, it is not so important to know precisely the location of these points, and the maximum strain amplitude nearly coincides with the strain amplitude in the transmitted wave.

Pressure on the Plate. The dimensionless hydrodynamic pressure on the plate is determined from the relation $p = -\rho(\varphi_t + g\eta_+)$ or $p = i(\varphi - \varphi_y)$. Substituting representation (4) for the potential into the last equation, we find the expression for the pressure on the plate:

$$p(x,0) = -i\beta\gamma^2 K_-(-\gamma)\sum_{j=-2}^{\infty} \mathrm{e}^{i\alpha_j x}\frac{\alpha_j^2 K_1(-\alpha_j)}{K_-(-\alpha_j)K_2'(\alpha_j)(\gamma-\alpha_j)}. \tag{8}$$

Here, as above, the main contribution is from the undamped wave with wavenumber α_0, while the remaining terms represent the edge effects decaying exponentially away from the edge.

The pressure amplitude in the transmitted wave p_∞ is linked to the corresponding potential amplitude $|T|$ by the relation $p_\infty = |K_1(\alpha_0)||T|$ and is calculated from the formula

$$p_\infty = \frac{2|K_1(\alpha_0)|}{\gamma+\alpha_0}\sqrt{\frac{\gamma|K_1'(\gamma)|}{\tanh(\alpha_0 H)|K_2'(\alpha_0)|}}.$$

Figure 5 shows the pressure amplitudes p_∞ versus β for various values of H. Here the effect of the liquid depth is significant. In a liquid of infinite depth, as $\beta \to \infty$, the pressure amplitude at infinity p_∞ tends to zero (to the pressure at infinity for an absolutely rigid plate). In a liquid of finite depth, the pressure at infinity tends to a constant because the pressure at infinity is finite for a rigid plate. As $H \to \infty$, this constant tends to zero.

The pressure amplitude at the edge p_0 is defined by the formula $p_0 = \Delta\eta$ (see Fig. 3). The liquid depth effect is significant for large values of β. Figure 6 shows distributions of pressure amplitudes over the plate for $H = 1$ and various values of β. As can be seen from Fig. 6, the pressure amplitude is nonmonotonic along x and reaches a maximum at the edge; as $x \to \infty$, it tends to a finite value that corresponds to the pressure amplitude

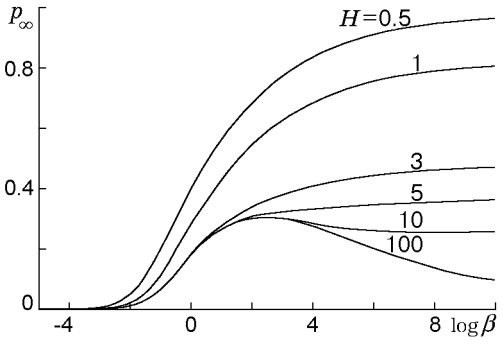

Fig. 5

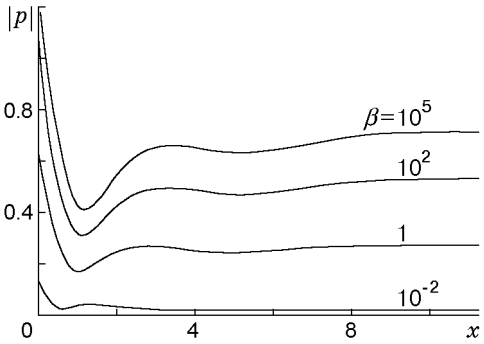

Fig. 6

Fig. 5. Pressure amplitudes p_∞ in the transmitted wave versus β for various values of H.

Fig. 6. Distributions of pressure amplitudes $|p|$ over the plate for $H = 1$ and various values of β.

in the transmitted wave. As $\beta \to 0$, the pressure tends to zero. Although, the absolute value of all terms of (8) decay monotonically with increase in x, the mismatch between the phases leads to nonmonotonicity of the pressure amplitude over x. The corresponding pressure distribution over the plate for an infinitely deep liquid is given in [8]. A comparison of the diagrams shows that the pressure amplitude distribution over the plate depends strongly on the liquid depth: as H decreases, the pressure amplitude increases.

This work was supported by the Foundation of Integration Programs of the Siberian Division of the Russian Academy of Sciences (Grant No. 1).

REFERENCES

1. V. A. Squire, J. P. Dugan, P. Wadhams, et al., "On ocean waves and sea ice," *Annu. Rev. Fluid Mech.*, **27**, 115–168 (1995).
2. A. V. Marchenko, "Flexural-gravity waves," in: *Tr. Inst. Obshch. Fiz. Ross. Akad. Nauk*, **56**, 65–111 (1999).
3. D. V. Evans and T. V. Davies, "Wave–ice interaction," Report No. 1313, Davidson Lab.–Stevens Inst. of Technol., New Jersey (1968).
4. V. V. Varlamov, "Scattering of internal waves by the edge of an elastic plate," *Zh. Vychisl. Mat. Mat. Fiz.*, **25**, No. 3, 413–421 (1985).
5. R. V. Gol'dshtein and A. V. Marchenko, "Diffraction of plane gravity waves at the edge of an ice sheet," *Appl. Math. Mech.*, **53**, No. 6, 924–930 (1989).
6. N. J. Balmforth and R. V. Craster, "Ocean waves and ice sheets," *J. Fluid Mech.*, **395**, 89–124 (1999).
7. L. A. Tkacheva, "Scattering of surface waves by the edge of a floating elastic plate," *Prikl. Mekh. Tekh. Fiz.*, **42**, No. 4, 88–97 (2001).
8. L. A. Tkacheva, "Diffraction of surface waves on a floating elastic plate," *Izv. Akad. Nauk, Mekh. Zhidk. Gaza*, No. 5, 128–141 (2001).
9. H. Suzuki and K. Yoshida, "Design flow and strategy for safety of very large floating structure," in: *Proc. of the Int. Workshop on Very Large Floating Structures* (Hayama, Japan, November 25–28, 1996), Part l (1996), pp. 21–27.